Available online at www.sciencedirect.com
ScienceDirect
Journal of Molecular Catalysis A: Chemical 256 (2006) 57–74
JOURNAL OF MOLECULAR CATALYSIS A: CHEMICAL
www.elsevier.com/locate/molcata

Interaction of water with titania and zirconia surfaces

Alexey Ignatchenko *, Donald G. Nealon, Roy Dushane, Keith Humphries

Chemical Technology Division, Eastman Chemical Company, Longview, TX 75607-7444, USA

Received 3 February 2006; received in revised form 2 April 2006; accepted 3 April 2006
Available online 5 June 2006

Dedicated to Prof. Ivan G. Bolesov on occasion of his 70th birthday.

Abstract

Isotopic exchange of water on the surface of monoclinic zirconia and the anatase form of titania was studied experimentally using an ordinary gas chromatograph/mass spectrometer (GC/MS) as a pulse microreactor. Interaction of water with these surfaces was modeled by first principles calculations for periodic structures within density functional theory. Experimental data support computational results showing dissociation of water on monoclinic zirconia's most stable surfaces ($\bar{1}$ 1 1), ($\bar{1}$ 0 1) and (1 1 1). Water is adsorbed molecularly on the anatase (1 0 1) surface and dissociatively on the anatase (1 0 0) surface. Interaction of water with the anatase (0 0 1) surface proceeds through insertion into a Ti—O bond. By monitoring the concentration of the mixed water isotope, DHO, during the isotopic exchange of surface water with D_2O, it was found that exchange of water on anatase surfaces at 200–400 °C proceeds by whole molecules from 30% to 70% depending on the temperature and the surface coverage. In contrast, water exchanges on zirconia by single hydrogen atoms with a complete scrambling of hydrogens, at least 99%, under the same conditions. The proposed mechanism of water exchange on zirconia surface includes interaction through hydrogen bonding between hydroxyl groups adsorbed on neighboring sites. The observed anomaly on anatase is in agreement with the preferential molecular adsorption on a (1 0 1) surface and with the insertion of water into Ti—O bonds on a (0 0 1) surface. This study contributes to the understanding of the atomic structure of acid–base catalytic sites on anatase titania and monoclinic zirconia surfaces.

Keywords: Hydrogen; Deuterium; Water; Chemisorption; Isotopic switch; Pulse microreactor

1. Introduction

Interaction of water with metal oxides plays an important role in catalysis [1–3], photo-catalysis [4,5], ceramics [6,7] and materials for the electronics industry [8]. Atomic scale details of the role of water in reaction mechanisms are essential for designing a family of heterogeneous catalytic processes such as the water gas shift reaction, combustion, hydration and dehydration of organic intermediates, ammoxidation, ketonization of carboxylic acids, photo-catalytic production of hydrogen from water, transformation of meta-stable crystallographic phases of metal oxides [6], etc. The ability to exchange hydrogen and oxygen between water and a catalyst surface affects both acid–base [1] and oxidation–reduction [3] properties of a catalyst. The amount and type of surface water is one characteristic of a catalyst that is related to its surface structure, polarity, hydrophilic or hydrophobic properties [9,10].

Water can be adsorbed on metal oxide surfaces either molecularly or in a dissociated form [11]. A conclusion on the state of water adsorption is often derived from infrared, Auger electron, X-ray photoelectron spectroscopy and temperature programmed desorption (TPD) experiments [3], i.e. under static conditions. In the meantime, the dynamic behavior of water on the surface during catalysis can be studied by the isotopic switch method, which is considered a more accurate reflection of the catalyst working conditions [12–14]. Despite an expanding use of isotopes for mechanistic studies in heterogeneous catalysis, only a single case is described in literature for the water exchange with metal oxide surfaces [15].

The anatase form of titania and monoclinic form of zirconia are examples of two different types of catalysts or catalyst supports with regards to their hydrophilicity, yet they are used in similar applications [8,16,17]. In our work we have not only

* Corresponding author. Present address: 321 Greenleaf Street, Longview, TX 75605, USA. Tel.: +1 903 445 9749; fax: +1 206 312 1622.
E-mail address: Alexey@mc-chem.com (A. Ignatchenko).

1381-1169/$ – see front matter © 2006 Elsevier B.V. All rights reserved.
doi:10.1016/j.molcata.2006.04.031

measured the adsorption capacity of water on zirconium and titanium metal oxides by the new method, but have also discovered unexpected details of the mechanism of isotopic exchange with the surface as a function of the type of metal oxide, temperature and the presence of cationic promoters. We believe this fundamental information on the dynamic behavior of water will provide a unique insight into the role of water in many heterogeneous catalytic reactions. Previously, such details were not available by static methods, like TPD, infrared or X-ray photoelectron spectroscopy.

We have also used computational studies to provide an explanation for the experimental facts. In recent computational work it was shown that water does not dissociate on the anatase (1 0 1) surface and it may only partially dissociate on the (0 0 1) surface [18]. To the best of our knowledge, first-principles computational studies of water interaction with monoclinic zirconia surface have not been done. The combination of experimental isotopic switch studies with a computational approach reveals details on water interaction with surfaces at an atomic level. This subject is of general interest to different fields of heterogeneous catalysis and materials sciences.

2. Experimental

2.1. Materials

Water–^{16}O normalized, ^{17}O- and ^{18}O-depleted, 99.99 atom% ^{16}O; water–^{18}O, normalized, 95 atom% ^{18}O; and deuterium oxide, minimum isotopic purity 99.99 atom% D, were purchased from Aldrich. Zirconia catalyst in monoclinic form was obtained from Saint-Gobain NorPro Corp. Titania catalyst in anatase form was obtained from Engelhard Corp. The BET surface area of catalyst samples was analyzed by Micromeritics Instrument Corp. Materials Analysis Laboratory. Untreated titania and KOH treated titania had 48 m^2/g and 42 m^2/g, respectively. Untreated zirconia and KOH treated zirconia had 52 m^2/g and 50 m^2/g, respectively. KOH treatment procedure followed by calcination resulted in a slight decrease in the surface area of both catalysts.

2.2. Catalyst preparation

Catalyst pellets, 100 g, were soaked in 100 mL of a 10% solution of KOH in water for 24 h at 60 °C under vacuum. The KOH solution was drained; the catalyst was washed with 100 mL deionized water three times, dried at 130 °C for 4 h, and calcined by heating to 450 °C at 1 °C/min rate and keeping at this temperature for 2 h. The calcined pellets were crushed, sieved, and the 0.25–0.71 mm particle size fraction was collected for use in water adsorption studies.

2.3. Isotopic exchange

An inside-gas chromatograph (GC) pulse microreactor was used as previously described [19]. A small amount of catalyst, 40 ± 1 mg, was placed inside a GC injection sleeve, in exactly the same place for all experiments, with the bottom of the catalyst bed 10 mm above the bottom of the injection sleeve. The catalyst bed was held in place by two pieces of glass wool on top and bottom. A typical catalyst bed size was 10–13 mm in length, and 2.0 mm in diameter. The length of the vaporization section was about 7–10 mm.

Isotopic exchange studies were performed using an Agilent Technologies model 6890 gas chromatograph equipped with an Agilent 5973 mass selective detector. Separation of the reactor products was performed on a J&W Scientific 30 m × 0.25 mm DB-5 capillary column. The chromatographic method used constant pressure, 11.9 psi (0.7 kg/cm^2), split ratio 40:1, helium carrier gas, column flow 1.4 mL/min and constant oven temperature (50 °C). The detector analyzed the mass range from 15 amu to 75 amu. The catalyst packed sleeve was inserted with a GC inlet temperature of 200–400 °C, and kept at this temperature for 10 min in helium 59 mL/min total flow before starting pulses. Time between pulses was 2.2 min.

2.4. Computation

Density functional calculations were performed using Materials Studio (DMol3 module) Version 2.2 software from Accelrys Inc. [20]. Electron exchange and correlation were described by the gradient corrected approximation based on the work of Perdew et al. publications [21].

Crystal structures were built based on lattice parameters published for monoclinic zirconia [22] and anatase [23] and adjusted by computing and minimizing their energy. Surfaces were cleaved to a depth 10–15 Å and the top two surface layers were allowed to relax, while the bottom layer was constrained. A vacuum slab of 10 Å thickness was built above the surface of the supercell constructed of 12 zirconium atoms and 24 oxygen atoms for ($\bar{1}$ 1 1), ($\bar{1}$ 0 1) and (1 1 1) monoclinic zirconia surfaces. Supercell constructed for anatase (1 0 1) and (0 0 1) surfaces contained 16 titanium and 32 oxygen atoms. A supercell for the anatase (1 0 0) surface contained 12 titanium and 24 oxygen atoms. All anatase surfaces had a 15 Å vacuum slab. Energy minimization was performed for the obtained supercell by density functional calculations using three different methods. In method 1, a DN basis set was used with a gradient corrected potential PW91 along with the standard parameters provided by the program, such as the medium integration accuracy and octupole multipolar expansion. Core treatment included effective core potentials. In two other methods, the DNP basis set and gradient corrected potentials, PW91 (method 2) and PBE (method 3) were used with the all electron relativistic option chosen for the core electrons treatment. Method 1 was always used first. The resulting geometry was re-optimized with method 2 and then with method 3. In all three methods, real space cutoff was 3.5 Å. The Brillouin zone was sampled by 2 × 4 × 1, 5 × 2 × 1 and 3 × 5 × 1 K-point set for anatase (1 0 1), (1 0 0) and (0 0 1) surfaces and by 3 × 3 × 1, 3 × 4 × 1 and 3 × 3 × 1 K-point set for ($\bar{1}$ 1 1), ($\bar{1}$ 0 1) and (1 1 1) monoclinic zirconia surfaces, respectively. For the orbital occupancy, 0.005 a.u. smearing was used. SCF density convergence, optimization energy convergence and gradient convergence were set to 0.00001 a.u., 0.00002 a.u. and 0.004 a.u., respectively. The same parameters were utilized for energy minimization with different adsorbates on the surface.

3. Results

3.1. Hydrogen–deuterium exchange

In this work, we have applied our recently developed pulse microreactor [19] for isotopic switch studies of water on the surface of zirconia and titania. Our method conveniently uses equipment already present in many modern laboratories and only trace amounts of isotopically labeled materials. A considerable amount of time and resources are saved when the catalytic reaction run and the analysis of products are combined into a single operation. The basic idea consists of placing a small amount of a catalyst inside the heated injection zone of a GC or GC/MS instrument and analyzing products generated through a series of injections. Thus, each injection of the starting material represents a pulse feed for the catalyst bed, generating products that are separated on the GC column and registered by the detector.

The catalyst surface was initially saturated with ^{17}O- and ^{18}O-depleted water–$H_2{}^{16}O$ by injecting 1.0 mkL of depleted water five times. This treatment was necessary to remove CO_2 adsorbed on surface from the atmosphere. Subsequently, D_2O was injected at 132 s intervals in the amount 0.1 mkL or 0.2 mkL until all hydrogens on surface were exchanged. Each peak was analyzed by mass spectrometry for the ratio of labeled to unlabeled water. A total disappearance of peaks with an odd *m/z* 17, 19 and 21 indicated that the catalyst surface was fully exchanged with the labeled water. The experiment was done at 200 °C and repeated at 300 °C and 400 °C each time with a fresh sample of titania and zirconia catalysts. An empty sleeve was also examined at all three temperatures and found to have negligible water adsorption effects and thus did not contribute to the measurements. An example of *m/z* 18, 19 and 20 fraction changes in the total area of water during pulse sequence is shown in Fig. 1. As can be seen during the isotopic switch, the fraction of the old isotope drops down while the new isotope fraction increases and the fraction of the mixed water, DHO, goes through a maximum. However, the fraction of *m/z* 18 does not decrease completely to zero, since it is associated both with H_2O and DO fragments. In order to find the degree of isotopic exchange, an accurate accounting of the deuterium fraction in the water peak is required. A deconvolution analysis to find exact fractions of all species was made for that purpose.

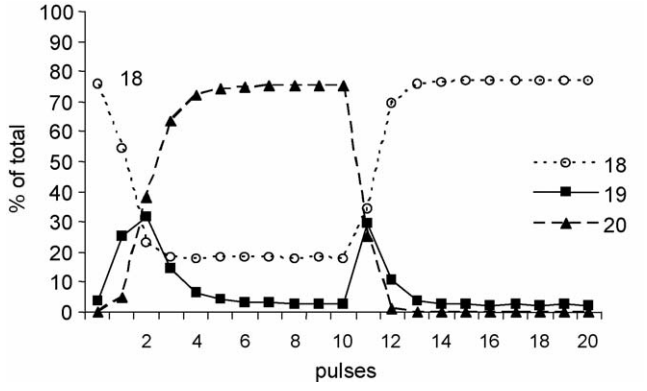

Fig. 1. Change of *m/z* 18, 19 and 20 fractions of the total amount of water during the switch from H_2O to D_2O and back to H_2O with titania catalyst at 200 °C.

Masses were assigned to the fragments as follows: 16 to O, 17 to OH, 18 to H_2O and DO, 19 to H_3O and DHO, 20 to D_2O and H_2DO, 21 to D_2HO and 22 to D_3O. Since some masses are common to different fragments, a contribution to their count from each fragment must be determined. Because a low resolution mass spectrometer (MS) was used, it was not possible to distinguish different fragments with the same mass, for example, H_2O from DO. However, it was observed from experiments described herein with unlabeled water that the ratio of *m/z* 18 to 17 abundance, which is due to the presence of H_2O or OH, is a constant equal to 3.78 under the current experimental conditions. In order to determine H_2O contribution to the *m/z* 18 counts, in all labeled injections the number of OH counts was simply multiplied by 3.78. Consequently, the remaining counts for the *m/z* 18 are a result of DO fragments. Similarly, the number of H_3O species was calculated by multiplying counts for unlabeled water, H_2O, by the factor 0.028. The latter factor could change based on the degree of self-ionization of water. For our experiments, it was accepted as a constant due to the consistency in the experimental conditions, such as the amount of material injected, ionization potential, carrier gas flow rate, etc. After subtraction of the H_3O counts from all *m/z* 19 counts, the number of DHO fragments was calculated. Like in the case of H_2O, the D_2O number was calculated from the number of DO fragments by multiplying with the factor 3.78. The H_2DO number was calculated by subtracting D_2O counts from *m/z* 20 counts. After all deuterium and hydrogen amounts were calculated, their ratio was used to find the degree of H/D exchange. Such deconvolution analysis gives more accurate results than just the ratio of *m/z* 19 and 20 counts to the sum of *m/z* 18, 19 and 20 counts used by authors of [15] in a similar experiment with magnesium oxide.

In order to find the proton capacity on the metal oxide surfaces studied, a purely statistical model for the proton exchange was considered. During the isotopic switch on a fully covered surface, the fraction, θ_i, and number, S_i, of new isotopes adsorbed on a sample after i injections are related as $\theta_i = S_i/N_o$, where N_o is the total number of both isotopes adsorbed on a sample (adsorption capacity of a sample at full coverage). We assume here that equilibrium is achieved during each pulse. This assumption is valid only if enough time is allowed for equilibration, for example, if at least 10 re-adsorption events occur per pulse. This requirement was verified by increasing the amount of injected deuterium oxide by 2 and 10 times. Since the calculated adsorption capacity did not change, our assumption is valid. In this case, a fraction of the new isotope atoms on the surface and in the gas phase are equal to each other and can be expressed as

$$\theta_{i+1} = \frac{S_i + G_{i+1}}{N_o + G_{i+1}},$$

where G_{i+1} is a number of new isotopes added into the gas phase with the injection $i+1$. After combining both equations, the adsorption capacity can be calculated as

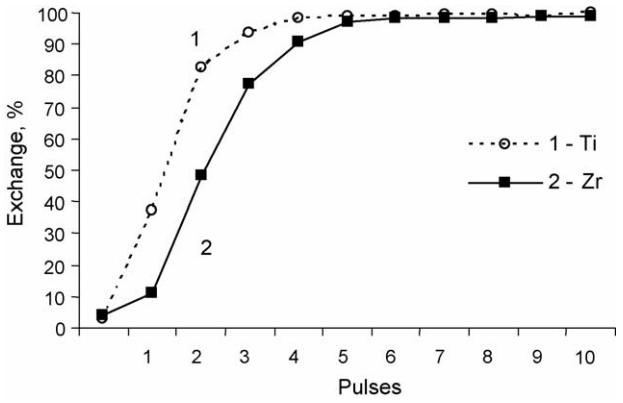

Fig. 2. H_2O–D_2O degree of exchange, θ_i, presented as %D, for titania (curve 1) and zirconia (curve 2) catalysts at 300 °C.

$N_o = G_{i+1} \times (1-\theta_{i+1})/(\theta_{i+1}-\theta_i)$, or

$$N_o = \frac{G_i \times \Phi_i}{-\Delta\Phi_i}, \quad (1)$$

where $\Phi_i = 1-\theta_i$ is the fraction of the old isotope, and $-\Delta\Phi_i = \Phi_{i-1} - \Phi_i$ is its loss.

A typical graph, showing the dependence of fraction θ_i on the number of pulses for titania and zirconia catalysts at 300 °C, is shown in Fig. 2. It can be seen that, in the case of zirconia, a higher number of pulses is required to reach a full exchange than for titania. This is due to a higher adsorption capacity of zirconia than titania.

Knowing the catalyst surface area and the amount of labeled water required for a full saturation of the surface, N_o, calculated by formula (1), the concentration of sites capable of water exchange on titania and zirconia was found at different temperatures (Fig. 3;Table 1). It should be noted that N_o can be calculated for any pair of sequential pulses. The results presented in Fig. 3 are mean values calculated within the range from 0% to 90% exchange.

We determined the adsorption capacity of water on anatase at temperatures from 200 °C to 400 °C to be 1.1–0.8 nm^{-2}, which is lower than the value of 1.9 nm^{-2} found by the TPD method [24], as would be expected. It should be understood that the TPD method is a relative measurement, showing the amount of adsorbed water lost between two different temperatures. Typically, the measurements are made at room temperature where the surface is saturated, and a higher temperature at which desorption is believed to be complete. Thus, the cumulative TPD amount characterizes adsorption at the temperature at which saturation is complete. Therefore, it is higher than the absolute value of the adsorption under equilibrium with a vapor phase at each specific temperature as measured by our method.

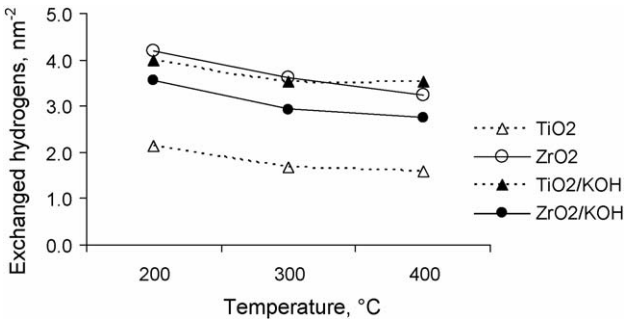

Fig. 3. Concentration of hydrogens, measured by H_2O–D_2O exchange at temperatures 200–400 °C on the surface of: (a) titania, (b) zirconia, (c) KOH treated titania and (d) KOH treated zirconia.

In general, a higher concentration of surface hydrogens was found on monoclinic zirconia than on anatase. However, after KOH treatment the water content increased on titania but decreased on zirconia. The different effect of KOH treatment may be speculatively assigned to the partial conversion of surface ZrOH groups into zirconate, ZrOK, thus decreasing the concentration of hydrogens. On anatase, KOH may insert into Ti–O–Ti bridges, to make TiOK and TiOH groups, which should increase the proton concentration by fixing additional hydroxyl groups on the surface.

3.2. Hydrogen scrambling and formation of the mixed water isotope, DHO

When monitoring formation of the mixed water isotope, DHO, we noted an unexpected experimental result. It was found that the isotopic scrambling was incomplete on anatase samples. There was a deviation of the observed DHO concentration from the statistically expected one. It appeared as if hydrogens were exchanging for deuteriums by pairs on the anatase surface. This is in contrast to the full scrambling observed on monoclinic zirconia.

Table 1
Degree of hydrogen scrambling, S (%), and concentration of scrambled and non-scrambled protons (atoms/nm^2) on the catalyst surface, measured by H_2O–D_2O exchange; concentration of exchangeable oxygens (atoms/nm^2) on the catalyst surface as measured by $H_2{}^{16}O$–$H_2{}^{18}O$ exchange

Catalyst	TiO_2			TiO_2–KOH			ZrO_2			ZrO_2–KOH		
	200[a]	300[a]	400[a]	200[a]	300[a]	400[a]	200[a]	300[a]	400[a]	200[a]	300[a]	400[a]
S (%)	70	55	30	86	66	57	99	99	99	99	99	100
Total H	2.14	1.7	1.58	4	3.52	3.54	4.2	3.62	3.22	3.56	2.92	2.76
Scrambled H	1.5	0.92	0.48	3.46	2.34	2.02	4.18	3.6	3.2	3.54	2.88	2.74
Non-scrambled H	0.64	0.76	1.1	0.54	1.18	1.52	0.02	0.02	0.04	0.02	0.04	0.02
Oxygens	0.85	0.99	1.66	1.03	1.61	2.68	0.86	1.19	1.58	1.13	1.68	2.32
H:O ratio	2.5	1.7	1.0	3.9	2.2	1.3	4.9	3.0	2.0	3.2	1.7	1.2

[a] Temperature.

Assuming that recombination of the dissociated water proceeds randomly, the concentration of water-19 during isotopic switch should be determined by the probability of forming mixed water, DHO, from D and H, versus forming two symmetrical waters, D_2O and H_2O. Since the probability of forming DHO is proportional to the concentration of both D and H, the corresponding probability function should go through a maximum as the concentration of H decreases, and the concentration of D increases. Consequently, the ratio between water isotopes 18, 19 and 20 may provide valuable information on the nature of water interaction with surfaces.

The simplest logical explanation for the observed anomaly is that the isotopic exchange is occurring by whole molecules of water rather than by single hydrogen atoms. This could be due to a number of reasons, one of them being non-dissociative adsorption which reduces the chance for the formation of the mixed water, DHO. The molecular form of adsorption may explain why the mixed water isotope is completely or partially missing in the desorbed vapors. We attempted to measure the observed anomaly quantitatively. Computations suggested that the interpretation may not only relate to the degree of water dissociation, but also to the specific way water interacts with the anatase surface. A detailed explanation is given in Section 5.

A mathematical approach to the problem can be reduced to the calculation of probabilities P_{18}, P_{19} and P_{20}, of forming water-18, -19 and -20 isotopes depending on the degree of hydrogen scrambling, S. An efficiency of exchange, F, is introduced as the factor showing what fraction of molecular water is actually participating in the exchange. A statistical model was built in an Excel spreadsheet, where the following formulas were used.

If the number of all isotopes, adsorbed on the surface consist of:

H	number of dissociated hydrogens
H^h	number of hydrogens remaining as non-dissociated H_2O
D	number of dissociated deuteriums
D^d	number of deuteriums remaining as non-dissociated D_2O
H^d	number of hydrogens remaining as non-dissociated DHO
D^h	number of deuteriums remaining as non-dissociated DHO (obviously, $D^h = H^d$)

and the number of deuterium atoms added for exchange as D_2O is D^{ad}, then the total number of isotopes, available for mixing, is

$$T = (H^h + D^d + H^d + D^h + D^{ad}) \times F + H + D,$$

and the probability of leaving single hydrogens on the surface is

$$P^h = S \times \frac{(H^h + H^d) \times F + H}{T}, \quad (2)$$

while the probability of leaving single deuteriums on the surface is

$$P^d = S \times \frac{(D^d + D^h + D^{ad}) \times F + D}{T} \quad (3)$$

The rest of the hydrogens and deuteriums are paired into different isotopes of water. The probability of pairing hydrogens and deuteriums into water is

$$P^{hh} = \frac{(1 - P^h)^2}{2 - P^h - P^d}, \quad \text{for water-18,} \quad (4)$$

$$P^{hd} = \frac{2 \times (1 - P^h) \times (1 - P^d)}{2 - P^h - P^d}, \quad \text{for water-19,} \quad (5)$$

$$P^{dd} = \frac{(1 - P^d)^2}{2 - P^h - P^d}, \quad \text{for water-20.} \quad (6)$$

Then, these isotopes are mixed with the water which did not participate in the exchange. The number of hydrogens and deuteriums from the water fraction, which did not participate in the exchange, is $L = (H^h + D^d + H^d + D^h + D^{ad}) \times (1 - F)$.

The combined number of paired hydrogens and deuteriums results in the number $R = N_o \times (P^{hh} + P^{dd} + P^{hd}) + L$.

The fraction of each water isotope, m/z 18, 19 and 20, registered in the gas phase at equilibrium is expressed as the ratio of the number of deuterium and proton isotopes in the corresponding water isotope to the total number R of deuterium and proton isotopes available:

$$P_{18} = \frac{P^{hh} \times N_o + H^h \times (1 - F)}{R} \quad (7)$$

$$P_{19} = \frac{P^{hd} \times N_o + (H^d + D^h) \times (1 - F)}{R} \quad (8)$$

$$P_{20} = \frac{P^{dd} \times N_o + (D^d + D^{ad}) \times (1 - F)}{R} \quad (9)$$

The developed model was applied to the experimental data. The degree of hydrogen scrambling on surface, S, and the efficiency of exchange, F, were optimized using the Microsoft Excel Solver tool[1] to match the calculated probability with the concentration of water isotopes found experimentally in each injection (some examples are shown in Fig. 4). During the optimization, the sum of standard deviations for each probability function was minimized by adjusting F and S. Data on water dissociation are shown in Table 1. The reported values of F and S are mean values for each exchange sequence.

We found that hydrogen is completely scrambled on zirconia at all temperatures with a high efficiency of exchange, 99%. Water adsorption on anatase proceeds with only partial hydrogen scrambling and with an exchange efficiency of approximately 86–97%. The degree of hydrogen scrambling depends on temperature, where it is higher at low temperatures and decreases with a temperature increase for both untreated and KOH treated

[1] The Microsoft Excel Solver tool uses the Generalized Reduced Gradient (GRG2) nonlinear optimization code developed by Leon Lasdon, University of Texas at Austin, and Allan Waren, Cleveland State University.

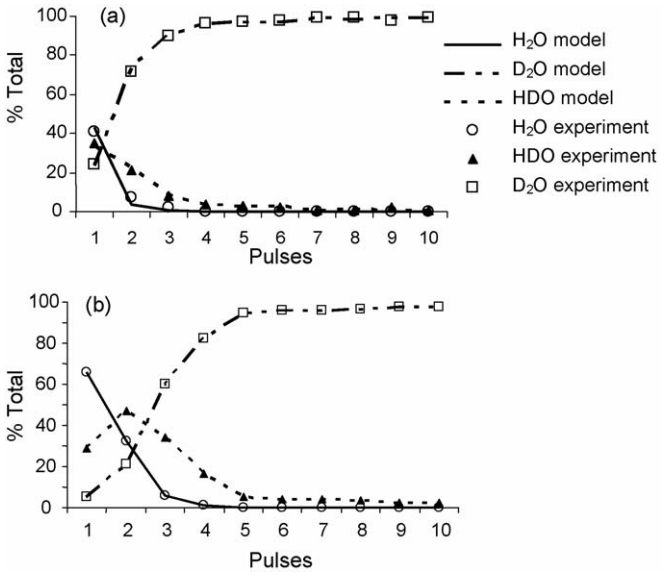

Fig. 4. H_2O/D_2O isotopic switch at 300 °C with: (a) titania and (b) zirconia.

titania. Also, a slightly higher degree of hydrogen scrambling on anatase was usually found at an earlier stage of the exchange sequence. A reverse exchange, i.e. the addition of $H_2{}^{16}O$ to the deuterated sample, gave approximately the same value for the adsorption capacity and the degree of hydrogen scrambling on both metal oxides.

The concentration of scrambled and non-scrambled hydrogens on anatase was estimated knowing the total concentration of hydrogen and the degree of hydrogen scrambling (Table 1). The overall concentration of hydrogens on surface is decreasing with the temperature increase, while the content of non-scrambled hydrogens appears to grow. This result may be interpreted as the H/D scrambling for the molecularly adsorbed water at lower temperatures, i.e. at a higher coverage, being due to the contacts made through intermolecular hydrogen bonding. At higher temperatures, hydrogen bonding between neighboring molecules of water is less probable due to a lower coverage. As a result, a lower degree of scrambling is found at higher temperatures. In addition, computational studies showed that the molecularly adsorbed water on anatase has a higher adsorption energy and should remain on surface longer than the dissociated one.

Anatase appears to be different from many other oxides studied in literature for which the binding energy of molecular water is lower than that of dissociated water [11]. As shown in Sections 4.4–4.6, water binds to the most common (1 0 1) surface of anatase in the molecular form stronger than in the dissociated one. Dissociative adsorption of water on the anatase (1 0 0) surface is only slightly preferred over a molecular form of adsorption. Water adsorption on an unreconstructed anatase (0 0 1) surface has the strongest energy among other surfaces and proceeds with insertion into Ti–O–Ti bonds. Even if water is formally considered to be dissociated, proton exchange on that surface may proceed by pairs due to the lack of hydrogen migration from the inserted water oxygen. On the (1 × 4) reconstructed anatase (0 0 1) surface, molecular adsorption of water again dominates over the dissociated form. Thus, on all anatase surfaces water hydrogens may be either exclusively or preferentially exchanged in pairs.

In addition, surface defects, such as a titanyl group, Ti=O, where two hydroxyls may attach to the same titanium atom may also contribute to the proton exchange by pairs. In this case, the exchange may proceed through dehydration and re-adsorption, $Ti(OH)_2 \rightarrow Ti{=}O + H_2O$, more slowly than the dehydration of two single hydroxyls on neighboring titanium atoms, $Ti(OH)–Ti(OH) \rightarrow Ti–O–Ti + H_2O$. The difference is that the single hydroxyl has several neighboring hydroxyl groups to engage in dehydration, and so, the formation of the mixed water, DHO, is possible, whereas this is less likely for the isolated $Ti{=}O \leftrightarrow Ti(OH)_2$ site. All of the above factors may contribute to the water exchange by hydrogen pairs observed experimentally.

It was particularly interesting to determine if there were changes for zirconia and titania resulting from KOH treatment. It was expected that single hydrogens might be substituted by potassium and thus become excluded from the exchange. The results showed this to be the case for zirconia (Table 1; Fig. 3). KOH treatment reduces the concentration of hydrogens on zirconia. An opposite effect is observed on anatase where the concentration of exchangeable hydrogens has doubled after KOH treatment (Table 1; Fig. 3). At the same time, the measured degree of hydrogen scrambling has increased slightly, so the majority of hydrogens created by KOH treatment on anatase are exchanged as single hydrogens. The number of hydrogens exchanged by pairs after KOH treatment increases with temperature. This amount is more likely assigned to the molecularly adsorbed water on the (1 0 1) surface of anatase, or to the water inserted into Ti–O–Ti bonds on the (0 0 1) surface. This conclusion is also supported by the oxygen exchange data.

3.3. Exchange of oxygen atoms

In order to elucidate the water exchange mechanism further, it is essential to know the ratio of exchangeable oxygens and hydrogens. In a separate series of experiments, we have studied $H_2{}^{18}O$ labeled water exchange by the same method (Table 1; Fig. 5). The amount of exchangeable oxygen grows with temperature for both metal oxides. For zirconia we found approximately a 2:1 ratio of hydrogens to oxygens exchanged at 400 °C, in accordance with the stoichiometry of the H_2O formula, while at 200 °C hydrogens are exchanged more readily as witnessed by their ratio to oxygens exceeding the stoichiometric 2:1 ratio. It seems that some oxygen atoms on the surface are not involved in the exchange at 200 °C, although they might be protonated. Their full exchange requires a temperature rise to 400 °C. The likelihood is that only mono-bridged oxygens, i.e. terminal OH groups, are exchanged at low temperatures, while protonated bi- or tri-bridged oxygens exchange at high temperatures.

On anatase, the ratio of exchanged hydrogens to oxygens is close to the stoichiometric value, 2:1, at low temperatures, but it changes to 1:1 when the temperature increases to 400 °C. This fact indicates participation of an extra oxygen atom from

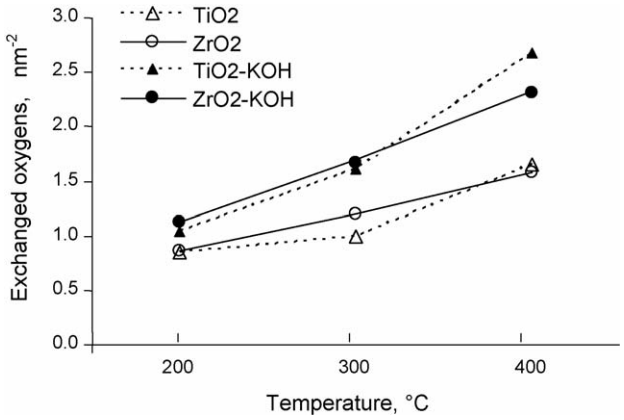

Fig. 5. Concentration of exchangeable oxygen atoms measured by $H_2{}^{16}O$–$H_2{}^{18}O$ exchange at temperatures 200–400 °C on the surface of: (a) titania, (b) zirconia, (c) KOH treated titania and (d) KOH treated zirconia.

the anatase lattice in the exchange at 400 °C. Its replacement requires higher energy compared to the oxygen atoms from water.

KOH treatment has increased the number of exchangeable oxygens on both metal oxides. Several possible explanations for the proton exchange by pairs on anatase have been discussed in the previous section. The mechanism that best satisfies oxygen exchange data is the insertion of water or KOH into the Ti–O–Ti bond on the anatase (0 0 1) surface which occurs more readily with increasing temperature. Another possibility for both metal oxides is the formation of potassium oxide as a separate phase which can add exchangeable oxygen atoms.

4. DFT computation modeling of water interaction with surfaces

In order to better understand the differences in the interaction with water between titania and zirconia, the structural and electronic properties of surfaces with adsorbed water were calculated according to the first principles density functional theory with periodic model using the DMol3 program.

Computational results in the literature support the non-dissociative mechanism of water adsorption on the most common (1 0 1) surface of anatase and only a partial dissociation on the (0 0 1) surface depending on coverage [18]. In contrast, we found that all three of the most stable monoclinic zirconia surfaces cause dissociation of adsorbed water at low coverage, below 25%. At a higher coverage, both molecular and dissociative adsorption may be present at the same time.

The most energetically preferred surfaces of monoclinic zirconia according to computational studies [25], ($\bar{1}$ 1 1), ($\bar{1}$ 0 1) and (1 1 1), were chosen for modeling in our work. Although it is ranked computationally as only the third most stable surface, the (1 1 1) termination of monoclinic zirconia is included in our work, since its existence is validated by HRTEM and FTIR experiments, at least for the samples sintered at high temperatures, 600–900 °C [26].

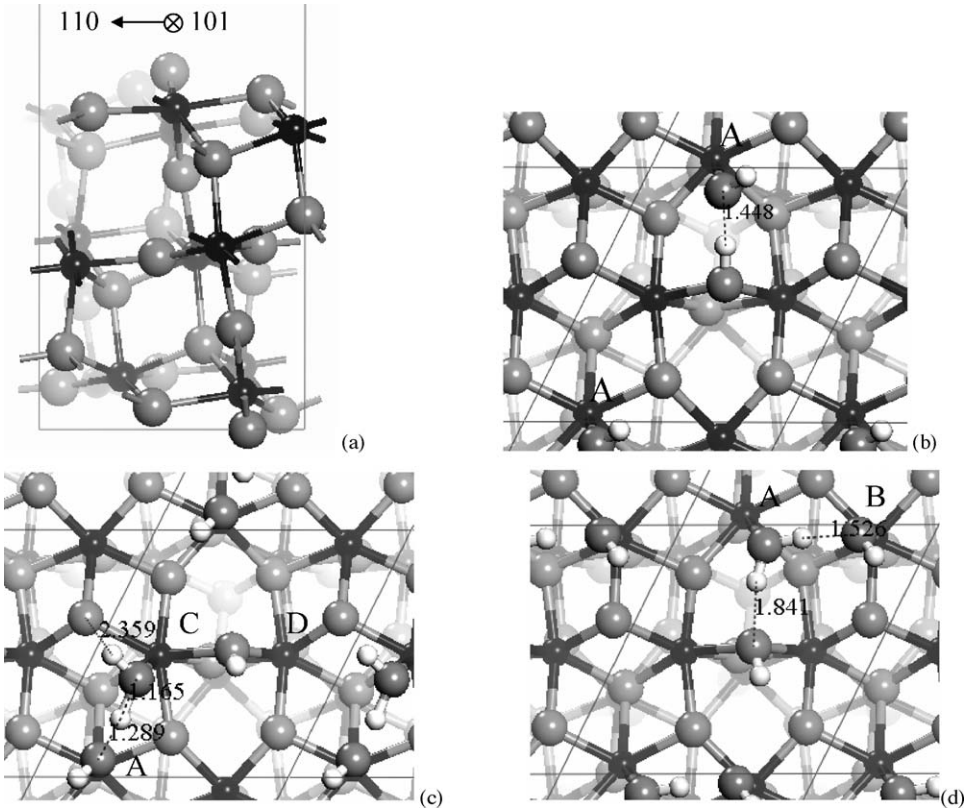

Fig. 6. Monoclinic zirconia ($\bar{1}$ 1 1). (a) Empty surface, side view. (b–d) Orthographic, top view. (b) Most favorable adsorption of water on site A representing 25% coverage proceeds with dissociation on proton and OH group. (c) Adsorption on sites AC, 50% coverage. (d) Adsorption on sites AB, 50% coverage. O atoms are large grey. Zr atoms are medium size, dark. H atoms are small light. Atoms in the background are shaded lighter. Hydrogen bonding is shown in dotted lines.

Details on the computational approach are described in Section 2. We have used three different methods. The first method, less accurate, but computationally inexpensive, was used in the search of the lowest energy structures. It uses a single effective potential for the core treatment and a double numerical set of valence atomic orbitals. Method 1 significantly overestimates adsorption energies. Calculations were repeated by two other methods for all surfaces and the most important adsorbate structures on them with a more accurate DNP basis set which included polarization p- and d-functions for all non-hydrogen atoms. Core treatment included all electrons explicitly with some relativistic effects. The latter two methods gave more accurate adsorption energies.

4.1. ($\bar{1}$ 1 1) monoclinic zirconia

The reported XRD lattice parameters for monoclinic zirconia [22] were optimized with the minimum found at +0.90% of the original length, resulting in $a = 0.5215$ nm, $b = 0.5279$ nm and $c = 0.5389$ nm.

Monoclinic zirconia is cleaved according to the set of rules discussed by Christensen and Carter [25]. A supercell is constructed from three layers, in which 12 ZrO_2 units were present (Fig. 6a). Cartesian coordinates of the bottom layer atoms are constrained, and two top layers are allowed to relax.

Examination of the resulting surface reveals four non-equivalent zirconium atoms, three of which are six-fold coordinated (6-c), marked as A, B and C, and the fourth one is seven-fold coordinated (7-c), site D (Fig. 6). Among 6-c Zr atoms, the ones at position C are closest to the surface, while those at position A are the deepest. There are four 3-c and one 2-c oxygen atoms at the surface. An upper case 1–3 letters index for oxygen atoms is used to show the number of connected Zr atoms and to which ones.

After performing surface relaxation we added molecules of water, one by one to all four different sites and minimized the

Table 2
Computed adsorption energies depending on water coverage for different sites on monoclinic zirconia and anatase surfaces

Entry	Adsorption site	Concentration of water (nm^{-2})	Coverage (%)	Type of adsorption	Adsorption energy (kcal/mol)			Figure
					Method 1[a]	Method 2[a]	Method 3[a]	
ZrO_2 ($\bar{1}$ 1 1) surface								
1	A	2.19	25.0	Dissociative	41.5 (1.8)	29.9 (1.30)	28.8 (1.25)	Fig. 6b
2	AC	4.38	50.0	A—dissociative, C—molecular	39.4 (1.71)	28.7 (1.24)	27.6 (1.20)	Fig. 6c
3	AB	–	–	A—molecular, B—dissociative	39.2 (1.70)	26.7 (1.16)	25.8 (1.12)	Fig. 6d
ZrO_2 ($\bar{1}$ 0 1) surface								
4	A	2.76	50.0	Dissociative	43.2 (1.87)	33.0 (1.43)	31.2 (1.35)	Fig. 7a
5	B	–	–	Dissociative	46.3 (2.01)	37.8 (1.64)	36.3 (1.57)	Fig. 7b
6	AB	5.51	100	B—molecular, A—dissociative	41.5 (1.80)	31.6 (1.37)	30.3 (1.31)	Fig. 7c
ZrO_2 (1 1 1) surface								
7	A	1.97	25.0	Dissociative	40.0 (1.73)	30.0 (1.30)	29.4 (1.27)	Fig. 8b
8	B	–	–	Dissociative	44.8 (1.94)	34.6 (1.50)	32.8 (1.42)	Fig. 8c
9	AB	3.93	50.0	A—molecular, B—dissociative	45.4 (1.97)	34.4 (1.49)	33.5 (1.45)	Fig. 8d
10	ABC	5.90	75.0	B, C—dissociative, A—molecular	39.0 (1.69)	27.4 (1.19)	26.4 (1.15)	Fig. 8e
TiO_2 (1 0 1) surface								
11	A	2.52	50.0	Molecular	28.4 (1.23)	19.4 (0.84)	19.6 (0.85)	Fig. 9a
12	AB	5.04	100	Molecular	27.8 (1.21)		19.3 (0.84)	Fig. 9b
TiO_2 (1 0 0) surface								
13	A	2.70	50.0	Molecular	23.5 (1.02)		17.2 (0.74)	Fig. 10a
14	A	–	–	Dissociative	29.8 (1.29)	18.8 (0.81)	17.8 (0.77)	Fig. 10b
15	AB	5.40	100	Dissociative	26.0 (1.13)		14.1 (0.61)	Fig. 10c
TiO_2 (0 0 1)								
16	A	3.39	50.0	Dissociative	45.3 (1.96)	41.0 (1.78)	39.9 (1.73)	Fig. 11
1 × 4 reconstructed TiO_2 (0 0 1)								
17	–	1.70	20.0	Molecular			18.2 (0.79)	Fig. 12a
18	–	3.40	40.0	Molecular			16.8 (0.76)	Fig. 12b
(1 × *n*) H_2O added TiO_2 (0 0 1)								
19	1 × 2	3.39	50.0	Dissociative			38.5 (1.67)[b]	–
20	1 × 3	2.26	33.3	Dissociative			62.4 (2.70)[b]	Fig. 13a
21	1 × 4	1.70	25.0	Dissociative			75.2 (3.26)[b]	Fig. 13b
22	1 × 5	1.36	20.0	Dissociative			85.5 (3.71)[b]	Fig. 13c
23	1 × 6	1.13	16.7	Dissociative			90.8 (3.94)[b]	Fig. 13d

The values in parentheses are in eV.

[a] See description of the computation methods in Section 2.

[b] Energy per mole of water. The energy per unit cell may be obtained by dividing the above values on the number *n* of unit cells in the supercell, which gives the energy values 19.2 kcal/mol, 20.8 kcal/mol, 18.8 kcal/mol, 17.1 kcal/mol and 15.1 kcal/mol for $n = 2$–6, respectively.

energy of the supercell containing adsorbed species. The results are summarized in Table 2. Adsorbed water was always oriented by its nucleophilic end toward the surface binding to one of the zirconium atoms. It was found that at ≤25% coverage, i.e. for the water concentration ≤2.19 nm^{-2}, molecular adsorption is not favored on any 6-c Zr sites, A, B or C, which is in good agreement with the experimental results.

The most preferred adsorption, site A, with the highest adsorption energy, 28.8 kcal/mol (method 3), is achieved by slightly shifting the OH group toward the O^{CD} oxygen and making a hydrogen bond with the dissociated proton which is attached to 2-c oxygen O^{CD} (Fig. 6b; Table 2, entry 1).

Adsorption of water on sites B and C is less strong, but it proceeds with dissociation as well, based on our results. The molecular adsorption on site B is 3.5 kcal/mol higher in energy and should not be favored. It was found that the dissociated proton prefers in both cases to stay on a 2-c oxygen O^{CD}, rather than on a 3-c oxygen.

Since the experimentally measured concentration of surface water at 200–400 °C is below 2.19 nm^{-2}, the 25% theoretical coverage used in our computational model is a valid representation of the hydrated surface for those temperatures. Both the experimental and the computational methods showed that the adsorption of water on zirconia at low coverage proceeds with dissociation. However, we were also interested to know what happens at higher coverages corresponding to lower temperatures, and at over-saturation of the surface, which may potentially occur during water exchange experiments.

At high coverage, above 25%, hydrogen bonding plays an increasingly important role in the stabilization of adsorbed water. We have studied adsorption of two molecules of water on three pairs of sites, AB, AC or BC, and also two molecules of water on just one site A (see Table 2, entries 2 and 3; Fig. 6c and d). The maximum energy released at 50% coverage is for the adsorption on sites AC and AB, 27.6 kcal/mol of water and 25.8 kcal/mol of water (method 3), respectively. In both cases, water adsorbed

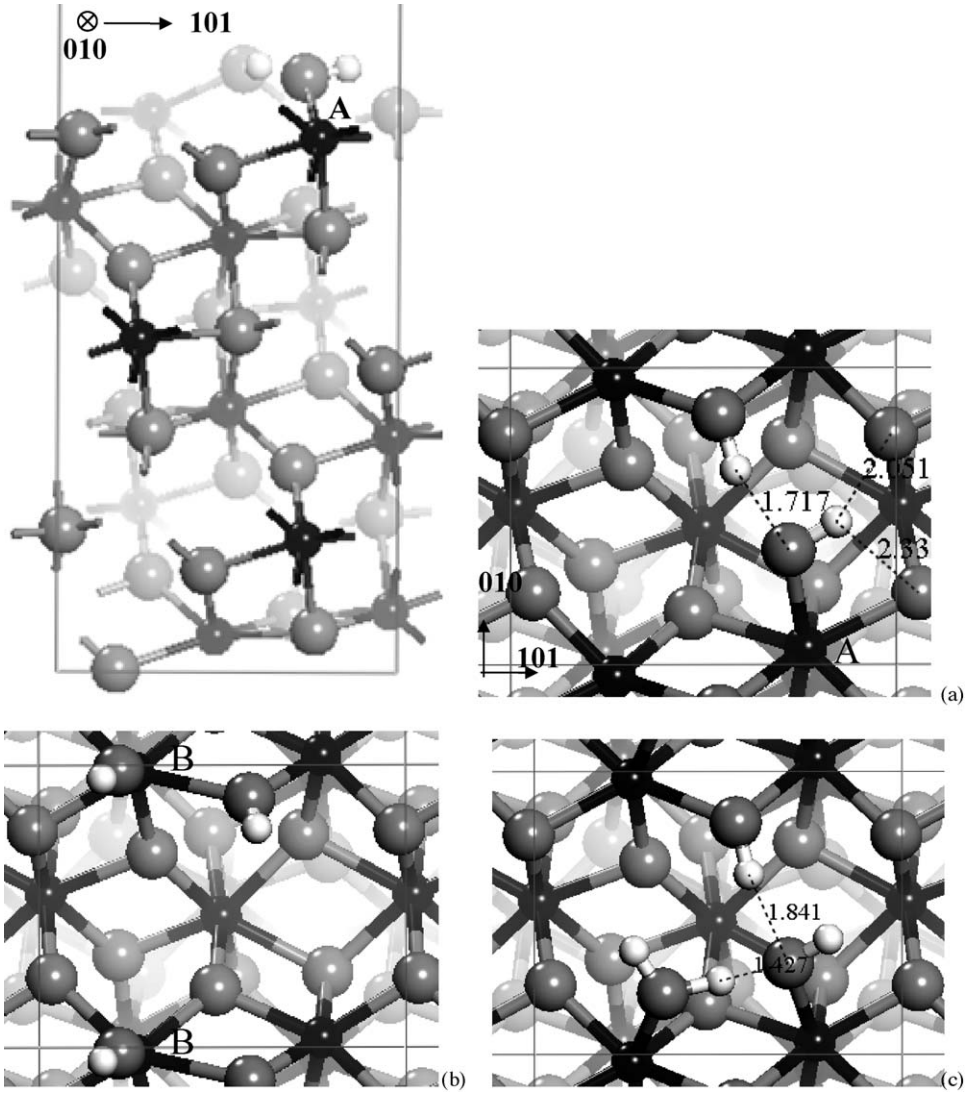

Fig. 7. ($\bar{1}$ 0 1) monoclinic zirconia surface. O atoms are large grey. Zr atoms are medium size, dark. H atoms are small light. Atoms in the background are shaded lighter. (a) Adsorption of one water molecule on site A, 6-c Zr, representing ≤50% coverage. (b) Adsorption of one water molecule on site B, 5-c Zr, representing ≤50% coverage. (c) Adsorption of two water molecules on sites A and B, representing ≤100% coverage.

on site A remains in the molecular state stabilized by hydrogen bonds, while adsorption on the second site proceeds with dissociation. A dissociated proton prefers to move to a 2-c oxygen O^{CD}. Adsorption of two molecules of water on site A was disadvantaged 7.7 kcal/mol (method 1), relative to the adsorption on sites AC. For the adsorption pair BC, one molecule on site C is dissociated, the other one on site B is not. Such an arrangement results in a 4.6 kcal/mol of water higher energy (method 1), than the more favorable pair AC. Although the model for pairs is shown as the molecular state, it is not a "pure" one. One of the OH bonds is stretched to 1.165 Å and can easily dissociate. Due to easy sharing of the proton involved in hydrogen bonding, it will show up as the dissociated one in isotopic switch experiments.

Among several possibilities for the adsorption of three molecules of water, i.e. 75% coverage, the most probable showed average adsorption energy of 32.2 kcal/mol of water (method 1). In the case of four molecules of water, this value had decreased to 30.1 kcal/mol (method 1). For 75% and 100% coverage, a water molecule adsorbed on site A remains in the molecular form and it is stabilized by two hydrogen bonds to lattice oxygens in a way similar to that found on the anatase (1 0 1) surface [18]. We believe the reason for the molecular adsorption of water at a high coverage on zirconia is the stabilization by hydrogen bonding.

4.2. ($\bar{1}$ 0 1) monoclinic zirconia

This is the second most stable surface of monoclinic zirconia and it should be seriously considered in modeling. There are two different adsorption sites A and B assigned to six- and five-fold coordinated zirconium atoms, respectively. Adsorption of one molecule of water, representing ≤50% coverage, proceeds with dissociation on either site (Fig. 7a and b). Adsorption on the 5-c Zr, site B, is stronger due to a lower coordinative satura-

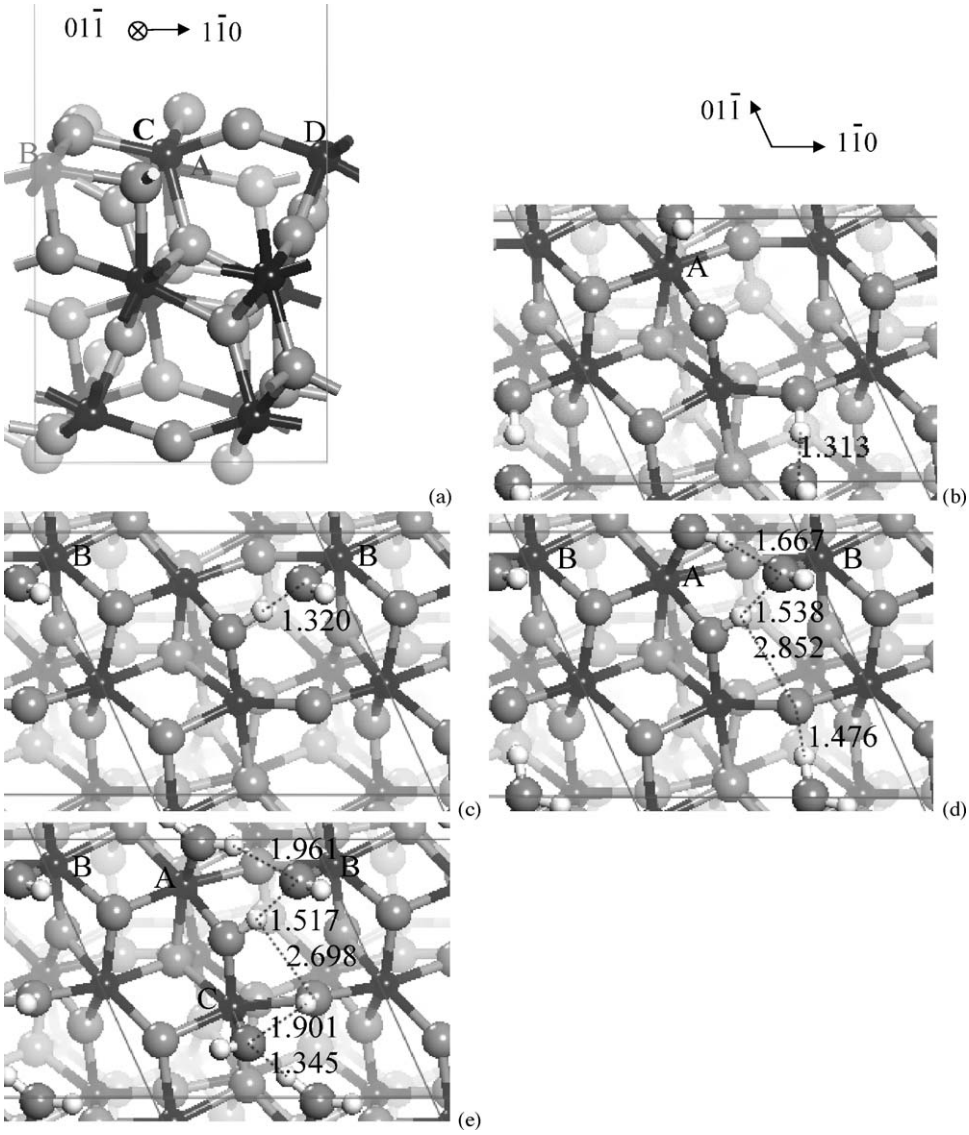

Fig. 8. Adsorption of water on (1 1 1) surface of monoclinic zirconia. O atoms are large grey. Zr atoms are medium size, dark. H atoms are small light. Atoms in the background are shaded lighter. Hydrogen bonding is shown in dotted lines. (a) Empty surface, side view. Adsorption on: (b) site A, ≤25% coverage, (c) site B, ≤25% coverage, (d) sites A and B, ≤50% coverage, and (e) sites A–C, ≤75% coverage.

tion of this atom (Table 2, entries 4 and 5), despite the fact that three hydrogen bonds are stabilizing adsorption on site A. Again, adsorption of two molecules of water representing 100% coverage is stabilized by hydrogen bonds between them as shown by dotted lines in Fig. 7c. One of the molecules may be considered as being adsorbed in the molecular state. However, it is clear that its proton forming the hydrogen bond can freely participate in the exchange as the single particle. Therefore, this water is likely measured as dissociated during the proton exchange experiments.

4.3. (1 1 1) monoclinic zirconia

The surface model has only six-fold coordinated zirconium atoms, each having a different oxygen environment (Fig. 8a and b). It is known there are two kinds of oxygen atoms in the bulk monoclinic crystal—three- and four-fold coordinated ones. Zirconium atoms in the monoclinic phase are always seven-fold coordinated. Each zirconium in the bulk is connected to four 4-c and three 3-c oxygens. Consequently, two kinds of six-fold coordinated zirconium atoms on the surface may be distinguished by the kind of oxygen atom they are missing, either a three- or four-fold coordinated one. Some researchers [27] have suggested that this is the basis for the existence of two IR stretching bands, as opposed to the explanation by Tsyganenko and Filimonov [28] that the bands arise from the mono- or tri-coordinated surface OH groups. In our model, zirconium on sites A and C is missing what in the bulk phase would be a 3-c oxygen atom, while sites B and D are missing a 4-c bulk oxygen atom. Since surface oxygens also become under-coordinated after cleavage, it represents an additional factor for creating non-equivalent zirconium sites on the surface. Namely, site C zirconium is connected to two 2-c surface oxygens, while site A Zr atom is connected to one 2-c surface oxygen, and sites B and D are connected only to 3-c oxygens (Fig. 8). This structural difference leads to the strongest adsorption of one molecule of water, i.e. at 25% modeled coverage, to the site B, 32.8 kcal/mol (method 3, Table 2, entry 8; Fig. 8c). The second strongest adsorption of a single water is on site A, with an adsorption energy 29.4 kcal/mol of water (method 3, Table 2, entry 7; Fig. 8b). However, adsorption of a pair of water molecules on neighboring sites A and B resulted in an even higher adsorption energy of 33.5 kcal/mol (method 3, Table 2, entry 9; Fig. 8d). According to our results, the preferred state of water adsorption is achieved by pairing molecules on sites A and B until they are filled in. Adsorption on sites C and D is strongly disfavored 20–25 kcal/mol (method 1). As one can see, there is no relation of the adsorption energy to the structural type of sites described above. Instead, the adsorption strength is determined by the existence of hydrogen bonds, which are created upon adsorption on sites A and B, but not on sites C and D. With the addition of more molecules, the average adsorption energy per mole of water drops appreciably (entry 10, Table 2).

4.4. (1 0 1) anatase

The initial lattice parameters for anatase from a low temperature neutron diffraction experiment [23] were optimized with the minimum found at +1.15% of the original length, resulting in $a = b = 0.3838$ nm and $c = 0.9644$ nm.

We have confirmed results obtained in [18] by Vittadini et al., showing that water does not dissociate when adsorbed on the (1 0 1) surface of anatase from 0% to 100% coverage. The adsorption energy calculated by our methods, 18.7–19.2 kcal/mol by method 3 (Table 2, entries 11 and 12), was slightly higher than 16.6–17.1 kcal/mol found earlier [18].

The structures of the adsorbed molecules representing ≤50% and ≤100% coverage are shown in Fig. 9. The anatase surface (1 0 1) is rather unique among other surfaces studied in our work. Molecules of water are fitting perfectly well in pockets between 5-c Ti and 2-c O. They are separated by 2-c oxygens and do not interact with each other. For this reason, the adsorption energy does not significantly depend on coverage. The reason for the preferred molecular adsorption on (1 0 1) anatase is the stabilization of water by hydrogen bonding to the lattice oxygen. Without such stabilization, water does dissociate on a structurally similar (1 0 0) surface.

4.5. (1 0 0) anatase

The constructed supercell contains 12 Ti and 24 O atoms. Two 5-c Ti, two 2-c O and two 3-c O atoms are at the surface (Fig. 10). A water molecule placed with its nucleophilic side above titanium atoms prefers to dissociate (see Table 2, entries 13 and 14) with the dissociated proton moving to the 2-c bridging

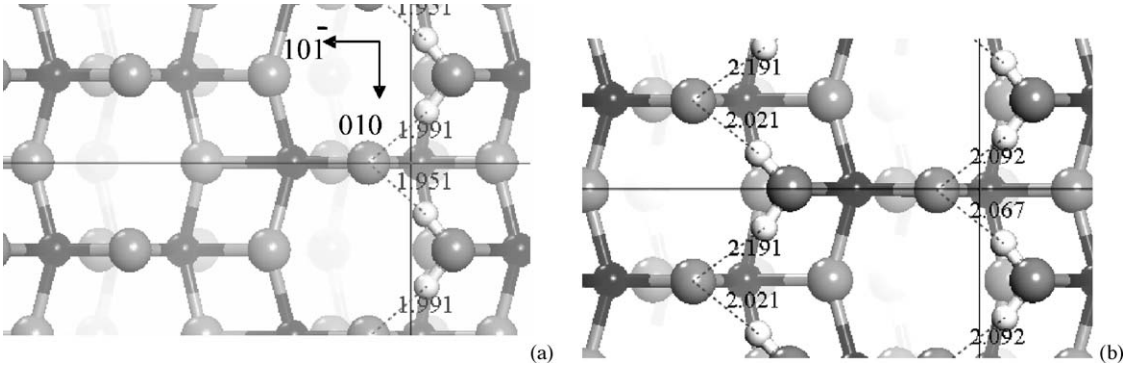

Fig. 9. Adsorption of water on anatase (1 0 1) surface. (a) ≤50% coverage and (b) ≤100% coverage. O atoms are large grey. Ti atoms are medium size, dark. H atoms are small light. Atoms in the background are shaded lighter. Hydrogen bonding is shown in dotted lines.

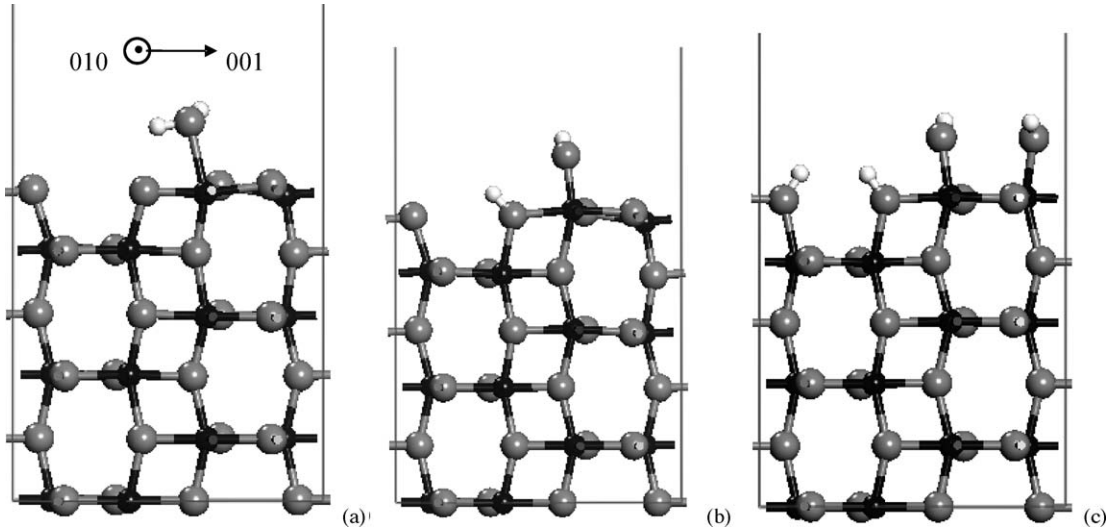

Fig. 10. Adsorption of water on anatase (1 0 0) surface. O atoms are large grey. Ti atoms are medium size, dark. H atoms are small light. (a) Molecular adsorption, 50% coverage; (b) dissociative adsorption, 50% coverage; (c) dissociative adsorption, 100% coverage.

oxygen. Hydroxyl oxygens are taking bulk-like oxygen positions (Fig. 10). The resulting OH groups do not interact with each other by hydrogen bonding, likely due to the long distances between them.

The difference between molecular and dissociative adsorption on an anatase (1 0 0) surface is very small, only ~0.6 kcal/mol (method 3). Vittadini et al. [18] mentioned without giving details that molecular water adsorption is preferred on anatase (1 0 0)/(010) surfaces according to their preliminary computational results. In conclusion, both forms of adsorbed water may equally exist on the anatase (1 0 0) surface.

4.6. (0 0 1) anatase

The constructed supercell contains two original unit cells in depth, 16 Ti and 32 O atoms. The resulting (0 0 1) surface has two equivalent 5-c titanium atoms on top, connected by two 2-c bridging oxygens in the (0 1 0) direction, and by two 3-c oxygens in the (1 0 0) direction (Fig. 11). A molecule of water interacts with the surface via insertion between titanium and 2-c oxygen atoms, representing 50% coverage (Fig. 11). The insertion results in shorter bonds between titanium and the second 2-c oxygen. The second molecule of water, as it was found in [18], does not insert as the first one. Instead, it is adsorbed as a non-dissociated molecule above the first one and stabilized by hydrogen bonding. The distinguishing feature of the anatase (0 0 1) surface is that titanium atoms do not change their coordination numbers after water adsorption, but retain their five-fold coordination. Adsorption energy on this surface is the strongest of the anatase surfaces studied in our work. The insertion model is in a good agreement with the experimental results for oxygen and proton exchange with water and should play an important role in representing anatase surface.

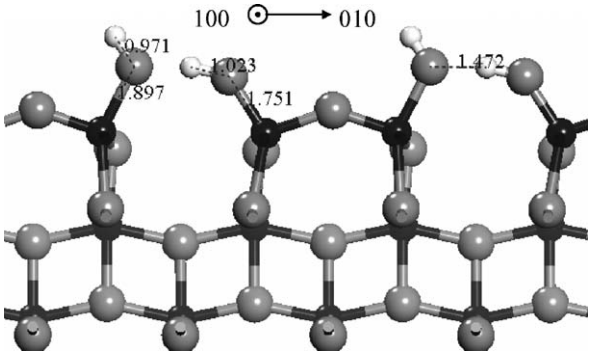

Fig. 11. Adsorption of water on anatase (0 0 1) surface at 50% coverage. O atoms are large grey. Ti atoms are medium size, dark. H atoms are small light. Atoms in the background are shaded lighter.

Recently, increased attention has been paid to a 1×4 reconstruction of the (0 0 1) surface of epitaxial anatase thin films [29,30]. The ad-molecule model for this reconstruction suggested by Lazzeri and Selloni [30] seems to explain experimental results [29] better than other models. We have studied the interaction of water with the 1×4 reconstructed (0 0 1) surface model of Lazzeri and Selloni and found that water is preferentially adsorbed at the ridge of the added TiO_2 rows, rather than at the valley between the added rows (Fig. 12). The adsorption energy, 18.2 kcal/mol (Table 2, entry 17), is comparable to that found on the other stable anatase surfaces, (1 0 1) and (1 0 0). Addition of the second molecule of water does not significantly decrease the average adsorption energy (16.8 kcal/mol, Table 2, entry 18) indicating an absent or a weak steric interaction between two molecules. The molecular state of the water adsorption on the reconstructed surface is preferred over the dissociated one.

We have also studied an alternative ad-molecule model in which water was added instead of TiO_2 to the original unreconstructed (0 0 1) surface in periodic $(1 \times n)$ rows. Different supercells with n original unit cells were constructed for this purpose and their energy was minimized with and without water (Fig. 13). The adsorption energy values per mole of water are shown in Table 2, entries 19–23. As noticed by Lazzeri and Sell-

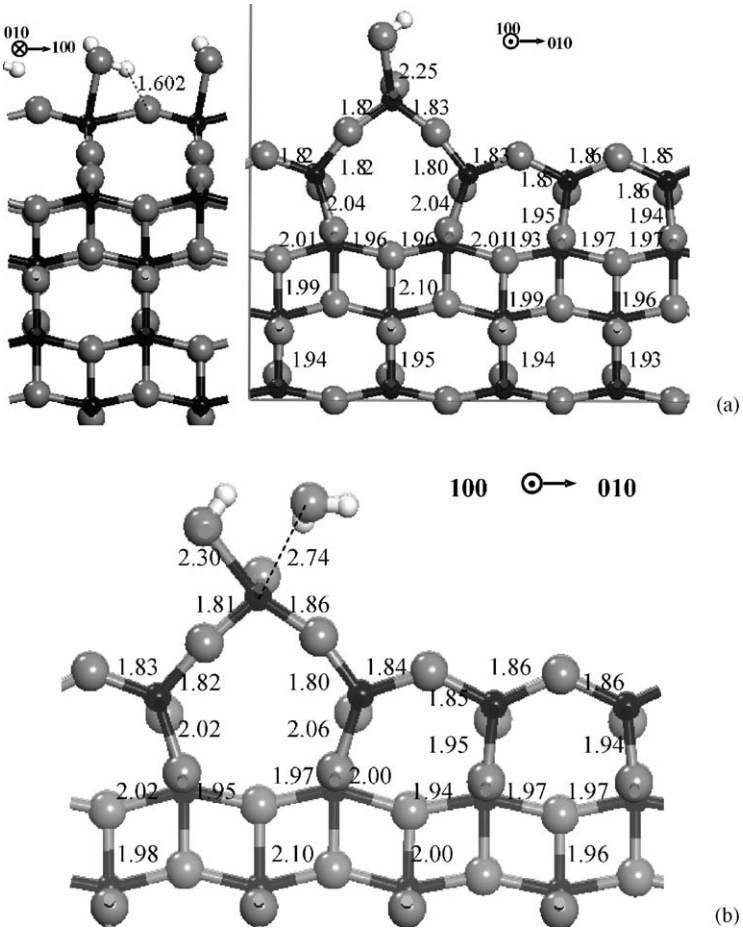

Fig. 12. Molecular water adsorption on a 1×4 reconstructed (0 0 1) anatase surface. (a) One and (b) two molecules of water adsorbed on the same titanium atom. O atoms are large grey. Ti atoms are medium size, dark. H atoms are small light.

oni, a large surface stress release is observed due to the shortage of Ti–O bonds caused by the insertion of an ad-molecule [30]. Water plays the role of the ad-molecule here, instead of TiO_2 in [30]. This effect becomes smaller with coverage, increasing from 16% to 50%, as indicated by the decreasing adsorption energy per mole of water. The surface energy of the hydrated periodic model of the (0 0 1) anatase surface goes through a minimum at $n = 3$, i.e. for (1×3) water insertion (Table 3). The hydrated surface energy, 0.33 J/m^2, in this case is slightly less than the 0.38 J/m^2 surface energy for the hydrated (1×4) reconstruction model. These computational results indicate that water, and perhaps some other molecules, can play a similar stabilization role for the (0 0 1) anatase surface as did the TiO_2 ad-molecule in the 1×4 reconstruction model suggested by Lazzeri and Selloni [30]. After submitting our work for publication, we have learned that the stabilization of the anatase (0 0 1) through hydration was also suggested in a computational study by Gong and Selloni [31].

Table 3
Calculated energies of hydrated (method 3) and non-hydrated surfaces (methods 1–3) of anatase and monoclinic zirconia (J/m^2)

Surface	Non-hydrated			Hydrated at different coverages (%)						
	Method 1[a]	Method 2[a]	Method 3[a]	16.7	20.0	25.0	33.0	40.0	50.0	75.0
(1 0 1) TiO_2	2.05	1.76	1.71	–	–	–	–		0.32	–
(1 0 0) TiO_2	2.39	2.13	2.09	–	–	–	–		0.40	–
(0 0 1) TiO_2	2.43	2.47	2.43	–	–	–	–		0.34	–
$(1 \times n)$ hydrated (0 0 1) TiO_2				0.39, $n = 6$	0.37, $n = 5$	0.35, $n = 4$	0.33, $n = 3$		0.34, $n = 2$	
1×4 reconstructed (0 0 1) TiO_2			1.87					0.38		
($\bar{1}$ 1 1) ZrO_2	2.73	2.45	2.40	–	–	0.45	–		0.36	–
($\bar{1}$ 0 1) ZrO_2	3.59	3.24	3.18	–	–	–	–		0.57	–
(1 1 1) ZrO_2	3.05	2.72	2.67	–	–	0.51	–		0.40	0.36

[a] See description of the computation methods in Section 2.

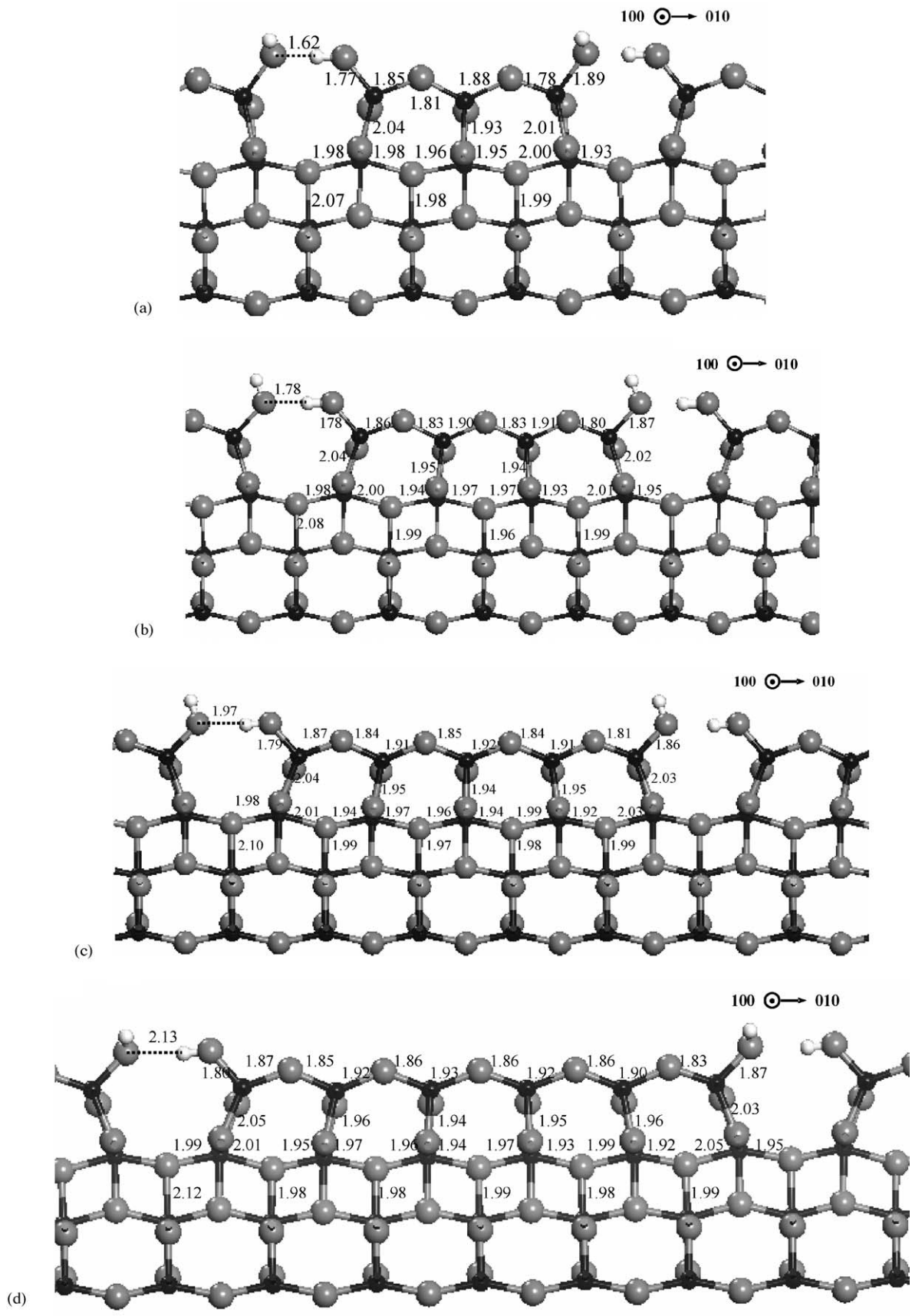

Fig. 13. $(1 \times n)$ periodic water insertion on a (0 0 1) anatase surface: (a) $n = 3$, (b) $n = 4$, (c) $n = 5$ and (d) $n = 6$. O atoms are large grey. Ti atoms are medium size, dark. H atoms are small light.

5. Discussion

A combined experimental and computational approach helped us to understand details of water interaction with zirconia and titania surface at an atomic level. We have found that water is adsorbed with its nucleophilic end bound to a coordinatively unsaturated metal cation on the surface of both metal oxides. At low coverage, the total energy minimum was generally obtained if water dissociates into OH and H groups on all studied monoclinic zirconia surfaces. The dissociated H moves to one of the lattice oxygens, preferentially to a bi-bridged one.

Various types of water adsorption on anatase surfaces, dissociative, non-dissociative and insertion, are found by computations. Experimental data on hydrogen scrambling during water exchange reflect contributions from different surfaces on anatase.

Traditionally, the molecular adsorption of water is related in literature to the physical form, as it has weaker adsorption energy. Thus, it was found that water is adsorbed on the anatase (1 0 1) surface below room temperature preferentially in the molecular state without dissociation [30]. TPD studies of water adsorption on anatase [32] in the 0–1000 °C temperature range showed two peaks, at 69–127 °C and 191–256 °C, assigned to physical and chemical adsorption, respectively. However, the shape of these two peaks [32] clearly shows some overlap, indicating both types of adsorption may co-exist in the 200–400 °C temperature range studied in our work. Infrared studies of water on an anatase surface suggest the presence of both hydroxyl groups and molecularly adsorbed water [33]. In addition, experiments show that all hydroxyl groups are exchangeable with D_2O even at 150 °C [33].

Hydrogen bonding plays a crucial role in the stabilization of adsorbed water on monoclinic zirconia at a high coverage when molecules are forced to make contacts due to the high concentration. However, whenever possible, hydrogen bonds are formed even at low coverage, thereby reducing the total energy. Hydrogen bond types can be classified into two categories: (1) between hydroxyl groups, normally formed at high coverage, and (2) between hydrogen of adsorbed water and lattice oxygen. In the literature, some evidence was presented for the interaction of surface hydroxyl groups on monoclinic zirconia [34]. According to Gerrato et al. [26], OH groups interact by hydrogen bonding with undissociated water rather than with other OH groups. Our most probable structures for water on zirconia ($\bar{1}$ 1 1) and (1 1 1) surfaces, shown in Figs. 6b and c, and 8c and d, can serve as examples of both types of such an interaction. As an exception, the most preferred adsorption state on the ($\bar{1}$ 0 1) zirconia surface does not have hydrogen bonds since its strength originates from an interaction with a highly under-coordinated zirconia atom. However, this surface has another adsorption site (Fig. 7a) where several hydrogen bonds help stabilize dissociated water.

In the case of titania, hydrogen bonding is observed experimentally in the IR spectrum for rutile, but not for anatase [35]. In agreement with this observation, our anatase models show the absence of hydrogen bonding between dissociated hydroxyl groups on the (1 0 0) surface (Fig. 10b and c). Conversely, it is found on the (1 0 1) surface for molecularly adsorbed water, which is stabilized by interactions with lattice oxygens (Fig. 9). Hydrogen bonding is also found for water insertion between Ti–O bond on the (0 0 1) surface (Fig. 11).

Since water helps to stabilize a surface, it would be interesting to compare the energy of the hydrated surfaces. We have calculated the energy of hydrated and non-hydrated surfaces as the difference between the total energy of the supercell with and without water and the energy of the equal amount of the bulk phase with and without water, divided by the area of the supercell surface. The results are shown in Table 3. Our energy is higher than reported in the literature [9,21] due to some differences in computational methods. However, relative stability of the surfaces is on the same order for anatase as determined by Lazzeri et al. [36]. For monoclinic zirconia, the ($\bar{1}$ 1 1) surface is the most stable termination based on our work and that of others [25]. We have found the (1 1 1) surface to be more stable than the ($\bar{1}$ 0 1) surface, in reverse order to that found for relaxed surfaces examined in reference [25], even though the energy difference between these two surfaces cited in [25] was very small. Hydration does not change that order for zirconium oxide (see Table 3). For titania, the highest energy of water adsorption on the (0 0 1) surface makes it the second most stable one when considering hydrated surfaces. However, with an increasing degree of hydration the difference in energy between surfaces becomes much smaller. The question of what surface may dominate in polycrystalline materials is more difficult to resolve. For example, if the preparation of a particular metal oxide is made in the presence of water by calcination of that metal hydroxide, the resulting microcrystalline particles may be distributed more equally among the different surface types than predicted computationally for non-hydrated surfaces. Therefore, it should be no surprise that higher energy surfaces may occasionally dominate in some cases, like the (1 1 1) surface studied in reference [26].

The theoretical concentration of zirconium atoms, and potentially, the concentration of water, is higher on a ($\bar{1}$ 1 1) surface, 8.76 nm^{-2}, and less on a ($\bar{1}$ 0 1) surface, 5.51 nm^{-2}. On a (1 1 1) surface there are 7.86 nm^{-2} zirconium atoms, so it can obtain a greater benefit from the stabilization by water than a ($\bar{1}$ 0 1) surface. The water concentration found experimentally by H/D exchange (Table 1) corresponds to 24% and 18% coverage for the ($\bar{1}$ 1 1) surface at 200 °C and 400 °C, respectively. For the ($\bar{1}$ 0 1) surface this would be 38% and 29% of the theoretical coverage.

Based on data in Table 1 and the theoretical concentration of titanium atoms, the anatase (1 0 1) surface would be 21% and 16% covered by water at 200 °C and 400 °C, respectively. Anatase (1 0 1) and (1 0 0) surfaces have comparable numbers of titanium atoms at the surface, 5.04 nm^{-2} and 5.40 nm^{-2}, while the (0 0 1) surface has a higher Ti atom density of 6.78 nm^{-2}. It would be covered at about 16% and 12% at 200 °C and 400 °C, respectively, if it was the only surface on the studied anatase samples. Most likely, anatase samples studied in our work have mainly (1 0 1) and (1 0 0) surfaces, with some (0 0 1) surface. Since the calculated adsorption energy, 39.9 kcal/mol, for the unreconstructed (0 0 1) surface is about two times higher than for the other two surfaces (Table 2, entries 11, 14 and

16), it should be hydrated more readily, with coverage close to 100%. The (1 0 1) and (1 0 0) surfaces should be hydrated to a lesser degree. However, if the (1 × 4) reconstruction observed on anatase (0 0 1) films [29] also takes place in powders, the extent of water coverage should be approximately equal on all three studied surfaces as their energies of water adsorption are comparable (see Table 2, entries 11, 14 and 17).

With increasing temperature, the dissociated, but more weakly bound, water on the (1 0 0) surface would be expected to desorb first, thus increasing the relative amount of non-dissociated water on the (1 0 1) and (1 × 4) reconstructed (0 0 1) surfaces which has a higher heat of adsorption and so, remains longer. This may serve as a supplementary explanation for the decrease in the degree of water dissociation observed with the temperature increase. As it has been discussed in Sections 3.2 and 3.3, the interaction of water with the unreconstructed anatase (0 0 1) surface may be one of the primary contributors to the same effect. According to the computations, water is formally dissociated on the (0 0 1) surface when inserted into Ti–O–Ti bonds (Fig. 11). However, interaction between neighboring molecules of water is restricted due to their separation on the surface by at least one Ti–O fragment. As a result, hydrogens may appear as non-scrambled in H/D switch experiments if the mechanism of its exchange includes desorption as the first step followed by re-adsorption. It is assumed that in the desorption step both hydrogens are departing together with one of the oxygens, to which they are attached, i.e. without scrambling on neighboring H or D. At the same time, the lattice oxygen can be exchanged as is evident from the water insertion structure in Fig. 11. The energy of water adsorption on the anatase (0 0 1) surface is the highest among other surfaces. It is logical to assume increasing participation of oxygen from the unreconstructed (0 0 1) surface in the exchange on anatase at higher temperature, which agrees well with the experimental data (Table 1). At high temperature and low coverage, the ratio of exchangeable oxygens and hydrogens is close to the ratio of 1:1 expected for the water insertion model on the (0 0 1) surface. The bridging oxygen, Ti–O–Ti, is "extracted" from the surface to participate in the exchange. The degree of hydrogen scrambling is low, due to the low coverage. Molecules of water are inserted into Ti–O–Ti bonds, and desorbed with little interaction between each other.

At low temperature, the coverage is higher and the chance of hydrogen scrambling due to the intermolecular contacts between molecules of water adsorbed on surface increases from 30% to 70% (Table 1). Short-lived structures of water formed during the exchange may include fragments of a second layer atop the first one as computationally predicted by Vittadini et al. [18]. In that case, water from the top layer may exchange hydrogens (deuteriums) with the bottom layer without exchanging oxygens. As a result, a higher ratio of exchangeable hydrogens to oxygens, 2.5:1, is observed at low temperature (Table 1).

KOH treatment breaks the symmetry in the water exchange by pairs of hydrogen. If potassium replaces one of the hydrogens pictured in Fig. 11 on the anatase (0 0 1) surface, it becomes clear how the exchange may proceed by single atoms. This is evidenced by the increase of the degree of hydrogen scrambling after KOH treatment by 11–27% (Table 1). In addition, KOH treatment seems to fix more water on anatase surfaces.

However, in contrast to anatase, all adsorption states of water found computationally on zirconia surfaces support a complete scrambling of hydrogens. The most evident is the case of preferred adsorption of water by pairs of molecules on the zirconia (1 1 1) surface which is stabilized by hydrogen bonding. Computational results suggest that hydrogen bonding is responsible for scrambling observed experimentally on zirconia. Experiments with zirconia show no deviation of the DHO concentration from the statistically expected value at the whole range of studied temperatures. The effect of KOH treatment on zirconia is also different. Since most water is dissociated on zirconia surfaces with the formation of hydroxyl groups, potassium may replace hydrogen in –OH groups and make surface –OK groups. This would explain the decrease in the concentration of hydrogens on zirconia measured after KOH treatment (Table 1).

Thus, water has a very different way of interacting with surfaces of the two metal oxides, anatase and monoclinic zirconia.

An interesting feature observed in the H/D isotopic switch experiments may help one to understand the exchange mechanism. A typical GC peak for water (Fig. 14a) is not symmetrical at the beginning of the exchange sequence. The previously adsorbed isotope of water elutes slightly earlier than the newly injected one. For example, when switching to D_2O, the GC peak for H_2O comes earlier than D_2O. The fact that this is not a chro-

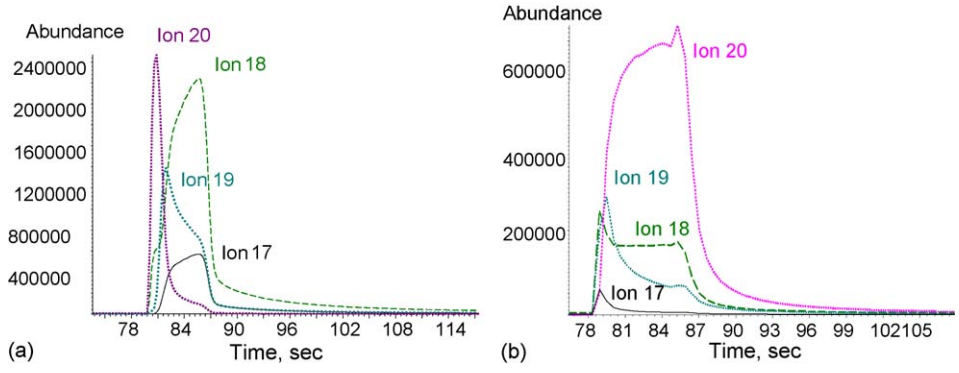

Fig. 14. (a) Observed distribution of isotopes in a typical GC water peak for isotopic switch study on a metal oxide. H_2O replaces D_2O. (b) Blank experiment without a metal oxide sample. D_2O replaces H_2O.

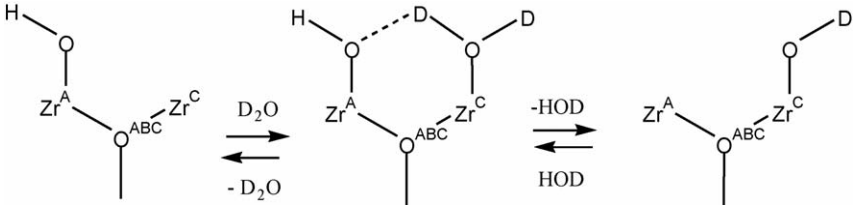

Scheme 1.

matographic separation of water isotopes on the GC column is proven by performing the exchange in reverse order, i.e. by saturating sample surface with D_2O and switching to H_2O. In this case, the D_2O peak comes before the H_2O peak. The observed effect is related to the change in the ratio of isotopes in the vapor cloud as it passes along the sample. We would like to demonstrate here that the asymmetry of the water peak is an expected phenomenon. For this purpose, we have modeled the course of exchange with a variable concentration of the new isotope in the cloud. We assume that the concentration of water should be the highest in the center of the vapor cloud and it changes according to the Gaussian (normal) distribution toward the edges. When the edge of the cloud reaches the sample, the exchange begins with a higher ratio of the old isotope to the new one. As the center of the cloud passes through the sample, the ratio changes in favor of the new isotope. Consequently, the beginning of the GC peak should have a higher concentration of the old isotope and the tail should have more of the new one (Fig. 15).

By comparing experimental results for oxygen and proton exchange with a zirconia sample, we are proposing an exchange mechanism via adsorption of water in excess to the thermodynamically equilibrated amount, followed by desorption of the excess.

This mechanism may be pictured, for instance, on a $(\bar{1}\,1\,1)$ surface by adsorption of a new water molecule to site C (Fig. 6c) in addition to an old one adsorbed on site A (Fig. 6b), followed by desorption of an old water from site A, resulting in the new molecule adsorbed on site C. Re-adsorption on site A and desorption from site C may be repeated, leading back to the more stable adsorption state A in Fig. 6b with the new water isotope. Obviously, hydrogens can be completely scrambled and the mixed water, DHO, can be formed according to the statistical law based on population of H and D. The proposed exchange mechanism is shown in Scheme 1.

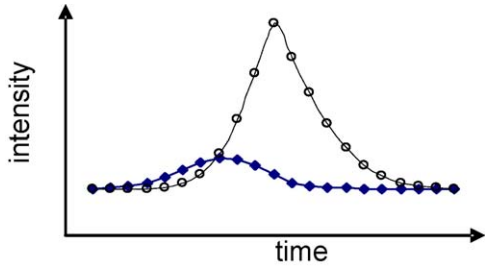

Fig. 15. Simulated GC water peak for the D_2O–H_2O switch experiments. It is assumed that the concentration of H_2O in the vapor cloud passing through the sample bed changes from the center to the edge of the cloud according to the Gaussian (normal) distribution. H_2O isotope: circles; D_2O: diamonds.

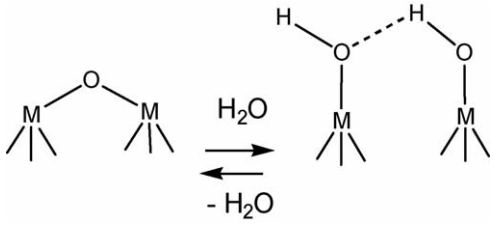

Scheme 2.

In a similar way, water may exchange on the other monoclinic zirconia surfaces, suggested by structures in Figs. 7c and 8d. In our opinion, the proposed mechanism is more credible for monoclinic zirconia than the widely used, but inadequate representation in Scheme 2. However, Scheme 2 may represent the interaction of water with the (0 0 1) surface of anatase (Fig. 11). Participation of the bridged oxygen atom from the anatase lattice in the hydration step is somewhat analogous to silica hydration [37].

6. Conclusions

A novel and convenient experimental method has been developed to find the degree of hydrogen scrambling for water adsorbed on the surface of metal oxides. This method provides a quick and easily available measurement of the mixed water concentration during the isotopic switch, from which one can elucidate the mechanism of the water exchange with the surface at the temperatures of interest.

DFT calculations for periodic structures predict water dissociation on the most important $(\bar{1}\,1\,1)$, $(\bar{1}\,0\,1)$ and (1 1 1) surfaces of monoclinic zirconia at low coverage. In contrast, adsorption is predicted to occur without dissociation on the major (1 0 1) surface and on the minor (1×4) reconstructed (0 0 1) surface of the anatase form of titania. Water does dissociate on the anatase (1 0 0) surface and interacts with the anatase (0 0 1) surface through insertion into Ti–O–Ti bonds. Upon desorption of water from the latter surface, the original Ti–O–Ti bonds restoration takes place without scrambling hydrogens at low coverage.

The combination of experimental data and computational analysis suggests that the interaction of water with titania and zirconia surfaces proceeds in different ways. The degree of hydrogen scrambling on the surface of monoclinic zirconia is very high, approximately 99%, and does not change with temperature within the 200–400 °C range. This is due to the mechanism of H/D exchange on monoclinic zirconia including water adsorp-

tion on neighboring cationic sites and exchange of hydrogens through hydrogen bonding.

The degree of hydrogen scrambling on anatase decreases from 70% to 30% with the temperature increase from 200 °C to 400 °C. Exchange of water without scrambling hydrogens is predicted by DFT computations for the next two models: (1) molecular adsorption of water on the anatase (1 0 1) surface and (2) insertion of water into Ti–O bonds on a (0 0 1) surface.

The authors believe that this approach can provide a new perspective into the dynamics of water interaction with metal oxide surfaces which will be helpful in understanding the many catalytic processes in which water is either directly involved or just present.

Acknowledgements

The help of Senior Statistician Michelle Holyfield and Computer Service Assistant Pamela Williams is greatly appreciated. We thank Eastman Chemical Company management for their permission to publish our work. Special thanks are extended to Mr. Jess Newsom for his support through the purchase of Materials Studio® software. We also thank Dr. Michael Sushchikh (University of California, Santa Barbara), Dr. Dawn Mason, Dr. Jerome Stavinoha and Dr. Ginette Tolleson for their critical suggestions during the preparation of this manuscript.

References

[1] H. Hattori, J. Jpn. Pet. Inst. 47 (2004) 67.
[2] M.A. Blesa, A.D. Weisz, P.J. Morando, J.A. Salfity, G.E. Magaz, A.E. Regazzoni, Coord. Chem. Rev. 196 (2000) 31.
[3] D.D. Beck, J.M. White, C.T. Ratcliffe, J. Phys. Chem. 90 (1986) 3123.
[4] A.L. Linsebigler, G.G. Lu, J.T. Yates, Chem. Rev. 95 (1995) 735.
[5] M.R. Hoffmann, S.T. Martin, W.Y. Choi, D.W. Bahnemann, Chem. Rev. 95 (1995) 69.
[6] X. Guo, Chem. Mater. 16 (2004) 3988.
[7] J.K. Lancaster, Tribol. Int. 23 (1990) 371.
[8] J.W. Fergus, J. Mater. Sci. 38 (2003) 4259.
[9] M. Kamei, T. Mitsuhashi, Surf. Sci. 463 (2000) L609.
[10] N. Sakai, R. Wang, A. Fujishima, T. Watanabe, K. Hashimoto, Langmuir 14 (1998) 5918.
[11] M.A. Henderson, Surf. Sci. Rep. 46 (2002) 1.
[12] Y.H. Hu, E. Ruckenstein, Acc. Chem. Res. 36 (2003) 791.
[13] A.M. Efstathiou, X.E. Verykios, Appl. Catal. A-Gen. 151 (1997) 109.
[14] S.L. Shannon, J.G. Goodwin, Chem. Rev. 95 (1995) 677.
[15] Y.-X. Li, K.J. Klabunde, Chem. Mater. 4 (1992) 611.
[16] L.M. Budin, L.M. Meyer, US Patent 6,858,768 to Conoco Phillips Company, Houston, TX (February 22, 2005).
[17] J.R. Sanderson, J.F. Knifton, E.T. Marquis, US Patent 5,414,163 to Texaco Chemical Inc., White Plains, NY (May 9, 1995).
[18] A. Vittadini, A. Selloni, F.P. Rotzinger, M. Gratzel, Phys. Rev. Lett. 81 (1998) 2954.
[19] A. Ignatchenko, J. Hill, J. Gray, D. Nealon, R. Dushane, Proceedings of 18th NACS Meeting, Cancun, 2003, p. 169.
[20] B. Delley, J. Chem. Phys. 113 (2000) 7756.
[21] (a) J.P. Perdew, Y. Wang, Phys. Rev. B 45 (1992) 13244;
(b) J.P. Perdew, K. Burke, M. Ernzerhof, Phys. Rev. Lett. 77 (1996) 3865.
[22] Y.D. McCullough, K.N. Trueblood, Acta Cryst. 12 (1959) 951.
[23] J.K. Burdett, T. Hughbanks, G.J. Miller, J.W. Richardson, J.V. Smith, J. Am. Chem. Soc. 109 (1987) 3639.
[24] F. Gonzalez, G. Munuera, J.A. Prieto, J. Chem. Soc., Faraday Trans. 174 (1977) 1517.
[25] A. Christensen, E.A. Carter, Phys. Rev. B 58 (1998) 8050.
[26] G. Gerrato, S. Bordiga, S. Barbera, C. Morterra, Appl. Surf. Sci. 115 (1997) 53.
[27] K.-H. Jacob, E. Knozinger, S. Benfer, J. Mater. Chem. 3 (1993) 651.
[28] A.A. Tsyganenko, V.N. Filimonov, J. Mol. Struct. 19 (1973) 579.
[29] R.E. Tanner, Y. Liang, E.I. Altman, Surf. Sci. 506 (2002) 251.
[30] M. Lazzeri, A. Selloni, Phys. Rev. Lett. 87 (2001) 266105-1.
[31] X.-Q. Gong, A. Selloni, J. Phys. Chem. B Lett. 109 (2005) 19560.
[32] M. Egashira, S. Kawasumi, S. Kagawa, T. Seiyama, Bull. Chem. Soc. Jpn. 51 (1978) 3144.
[33] M. Primet, P. Pichat, M.-V. Mathieu, J. Phys. Chem. 75 (1971) 1216.
[34] J. Erkelens, H.Th. Rijnten, S.H. Eggink-Du Burck, Recl. Trav. Chim. Pays-Bas 91 (1972) 1426.
[35] A.A. Tsyganenko, V.N. Filimonov, Usp. Fotoniki 4 (1974) 51.
[36] M. Lazzeri, A. Vittadini, A. Selloni, Phys. Rev. B 63 (2001) 155409.
[37] E.F. Vansant, P. Van Der Voort, K.C. Vrancken, in: B. Delmon, J.T. Yates (Eds.), Studies in Surface Science and Catalysis, vol. 93, Elsevier Science Publishers, NY, 1995.